Lasers in Manufacturing Conference 2021

Determination of thermophysical process limitations for the laser-based droplet brazing process using different droplet and substrate materials

Jakob Ermer[a,c,*], Florian Kohlmann[a], Markus Müller[a], Florian Kaufmann[a], Stephan Roth[a,c], Michael Schmidt[a,b,c]

[a] *Bayerisches Laserzentrum GmbH (blz), Konrad-Zuse-Straße 2/6, 91052 Erlangen, Germany*

[b] *Institute of Photonic Technologies (LPT), Friedrich-Alexander-Universität Erlangen-Nürnberg, Konrad-Zuse-Straße 3/5, 91052 Erlangen, Germany*

[c] *Erlangen Graduate School in Advanced Optical Technologies (SAOT), Paul-Gordan-Straße 6, 91052 Erlangen, Germany*

Abstract

The demand for microelectronic components is rising constantly over the last few decades due to the progress in digitalization. Along with this, the requirements for joining technologies are growing since they are highly responsible for progress in microelectronics. Laser-based droplet brazing shows unique features like a quasi-force-free joining process and high-temperature stable connections and is therefore on the way to its industrial implementation. While the first developments have been limited to contacting silver metallizations on piezo actuators, today the transferability of the process with regard to different brazing and substrate materials is a major goal. In this work the relation between the solidification time of the droplet and diffusion processes depending on the substrate layout and material properties is investigated via highspeed imaging and EDX analysis. Based on the thermophysical behaviour of the process, the scalability for future applications can be derived for different material combinations.

Keywords: micro joining; droplet brazing; electronic production; highspeed imaging

1. Introduction

The idea of detaching liquid metal droplets on different substrates has long been knownand has been researched for decades [1][2]. Up to now, there have been multiple attempts to generate droplets from

* Corresponding author.
E-mail address: j.ermer@blz.org.

different materials in different ways. The approaches range from melting from wire [3], metal foils [4] to single brazing spheres that are ejected from a capillary. Successful attempts to generate liquid metal droplets from spherical preforms have been carried out with W/Co capillaries [5]. These capillaries showed good results for melting soldering materials like SAC 305, which made it possible to establish this process on an industrial scale [6], [7]. This technology has been exclusively used for soldering and not for brazing droplet sphere materials and therefore further investigations have been carried out to enhance the possibilities of the technology for future applications. For contacting piezoelectric actuators it was necessary to develop a new process, where melting temperatures higher than 660°C were required for the joint, due to the subsequent aluminum die-casting process [5], because conventional laser soldering processes would not work [8]. Therefore, the brazing material was changed to CuSn11 and the W/Co capillary was changed to Al_2O_3, since it was found out, that the wetting susceptibility between CuSn11 and Al_2O_3 is comparably low. Influences of different capillary shapes were evaluated regarding gas flow fields and their overall influence on the process performance. With these measures it was possible to create joints on thin Ag-metallizations with thicknesses less than 20 µm on low temperature cofired ceramics [9] [10] [11]. The general performance of the process and the reliability of the created joints could be shown for a limited range of materials and joint designs [12][13].

The general transferability of the process was not investigated up to now, neither regarding the substrate material nor the brazing sphere material. Since each brazing process is mainly limited by the diffusion between the joining partners, temperature and time are the most relevant parameters besides metallurgical compatibility and wetting behavior. Due to the fact, that the maximum thermal energy $Q_{\text{thermal droplet,max}}$ of one droplet sphere is limited by its mass m_{droplet}, vapour temperature $T_{\text{vapour,droplet}}$ and heat capacity $c_{\text{p,droplet}}$ (see formula 1) the time for solidification on a certain substrate and therefore the time where an effective diffusion process takes place is limited by the thermodynamic properties and geometry of the substrate.

$$Q_{\text{thermal droplet,max}} = m_{\text{droplet}} \cdot c_{\text{p,droplet}} \cdot T_{\text{vapour,droplet}} \quad (1)$$

In the scope of this paper the influence of different substrate materials and their thickness is investigated regarding the resulting solidification times und shear strengths depending on the droplet-substrate combination.

2. Experimental Setup

For the laser-based droplet brazing process a single-mode fiber laser (IPG YLR-200 SM-WC) was used with a wavelength of λ_{laser} = 1070 nm. The laser beam is focused with a lens with a focal length of f_{Lens} = 50 mm. The resulting theoretical beam diameter is 11.4 µm at a raw beam diameter of 6.9 mm and a beam quality of M^2= 1.15. The laser beam is focused through a window into a process chamber by a motorized focusing lens to change the focal position of the laser beam relative to the brazing sphere.

To stop laser irradiation as soon as the droplet is ejected from the capillary, a photodiode is used to detect the leaking laser wavelength through the capillary as soon as the droplet detaches. For this purpose, a Si-detector is installed in combination with a bandpass filter for 1000-1100 nm and a neutral density filter (ND.2.0) to suppress irradiance from the surrounding.

For highspeed imaging a camera (Microtron EoSense mini 2) at a maximal resolution of 288 x 292 pixels at 10000 frames per second and a Navitar 12 x objective was used with a low-pass-filter at 1000 nm to block laser light coming from the process zone. For irradiation a white-light led source was used with a customized focusing setup.

The process flow can be divided in the following steps:

- inserting droplet sphere into the Al_2O_3 capillary
- applying of inert gas overpressure (N_2)
- irradiation of the droplet sphere with defocused laser beam
- melting of the droplet sphere in the capillary
- ejection of the liquid droplet by applied overpressure
- stop of laser irradiation and gas overpressure by diode signal

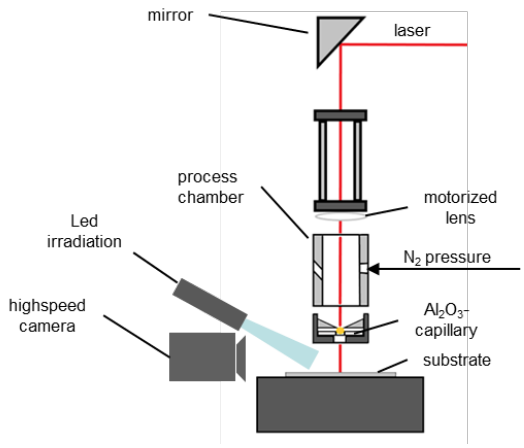

Fig. 1: Experimental setup for highspeed imaging of the laser-based droplet brazing process to determine flight and solidification times

3. Materials and characterization

3.1. Substrate materials

The substrate materials used for the experiments are listed in Table 1. For each material different thicknesses have been investigated. The thicknesses range from 0.025 – 0.2 mm. For contacting the foils, they were cut in sizes of 25 x 25 mm and fixed on a rectangular frame with an inner size of 20 x 20 mm to minimize heat conduction losses to surrounding materials.

Table 1: Thermophysical properties at room temperature for different substrate materials used for testing

Material	Density (kg/dm^3)	Liquidus temperature (°C)	Heat conductivity (W/(m·K))	Thermal expansion coefficient ($10^{-6}/K$)	Specific heat capacity (J/(g·K))	Electric conductivity ($m/(\Omega \cdot mm^2)$)
Al	2.70	660	235	23.8	0.897	37.7
Cu	8.96	1083	403	16.2	0.385	58.1
Ni	8.90	1455	91	13.3	0.444	13.9
Ag	10.49	960	430	18.9	0.235	61.35

3.2. Brazing materials

For the brazing spheres two different materials are investigated in the scope of this work. Most relevant physical data for the tin bronze (CuSn11) and pure silver (Ag) are shown in Table 2.

Table 2: Different materials at room temperature of droplet spheres used during the experiments

Material	**Density (kg/dm³)**	**Liquidus temperature (°C)**	**Heat conductivity (W/(m·K))**	**Thermal expansion coefficient (10^{-6}/K)**	**Specific heat capacity (J/(g·K))**	**Electric conductivity (m/(Ω·mm²))**
CuSn11	8.74	826.3 – 986.26	59	17.0	0.367	9.98
Silber	10.49	960	430	18.9	0.235	61.35

3.3. Process parameters for laser-based droplet brazing

For the experiments, that have been carried out the brazing spheres were irradiated with a beam diameter of 155 µm. The beam diameter was chosen smaller ($d_{laser,\ CuSn11}$ = 155 µm, $d_{laser,Ag}$ = 11.4 µm) than the sphere diameter to prevent unwanted energy input in the Al_2O_3 capillary. The laser power was kept on a constant level of $P_{Laser,CuSn11}$ = 100 W (continuous wave) for melting the CuSn11 spheres in the capillary. This set of parameters was identified as a stable combination in previous investigations. For the Ag spheres there was a higher power required ($P_{laser,Ag}$= 150 W) due to higher reflectivity at the infrared wavelength, this parameter set has not been investigated before.

The process gas for the experiments was nitrogen 5.0 with a constant overpressure of 75 mbar. The capillary has a thickness of 0.63 mm and is designed in a conic shape with a larger diameter of 0.63 mm and a smaller diameter of 0.57 mm. The working distance between capillary outlet und substrate surface was kept constant on 1.0 mm.

3.4. Determination of shear stress

To determine the maximum shear force F_{shear} tests were carried out according to DIN-EN 62137 1-2. The speed of the shear chinsel was set to 0.5 mm/s. The area $\mathrm{A}_{\mathrm{shear}}$ of the sheared droplet was measured via a stereoscopic microscope and an evaluation algorithm based on an ImageJ script. The shear stress τ_{shear} was calculated by formula 2:

$$\tau_{\mathrm{shear}} = \frac{F_{\mathrm{shear}}}{A_{\mathrm{shear}}} \tag{2}$$

4. Results and Discussion

In the following the most relevant results regarding highspeed imaging, shear testing and metallographic results will be presented and discussed afterwards.

4.1 Determination of solidification times by highspeed imaging

To determine flight time and the solidification time of the droplet spheres on different substrate materials the highspeed images are evaluated, as can be seen in Figure 2. At 0.0 ms the molten droplet is barely visible at the exit of the capillary and is ejected from the capillary until it hits the surface of the substrate material after 1.2 ms. Slight changes of the shape of the droplet sphere can be observed until 3.0 ms. After 3.0 ms a change of the roughness on the surface of the droplet is visible, which can be related to the solidification process and the phase transition from liquid to solid state. The solidification starts from the substrate surface to the upper braze surface and stops at the highest point of the braze sphere 6.6 ms after detachment from the capillary. The time difference between the visible stop of solidification at 6.6 ms and the first contact after 1.2 ms is defined as the solidification time of the droplet on the substrate surface.

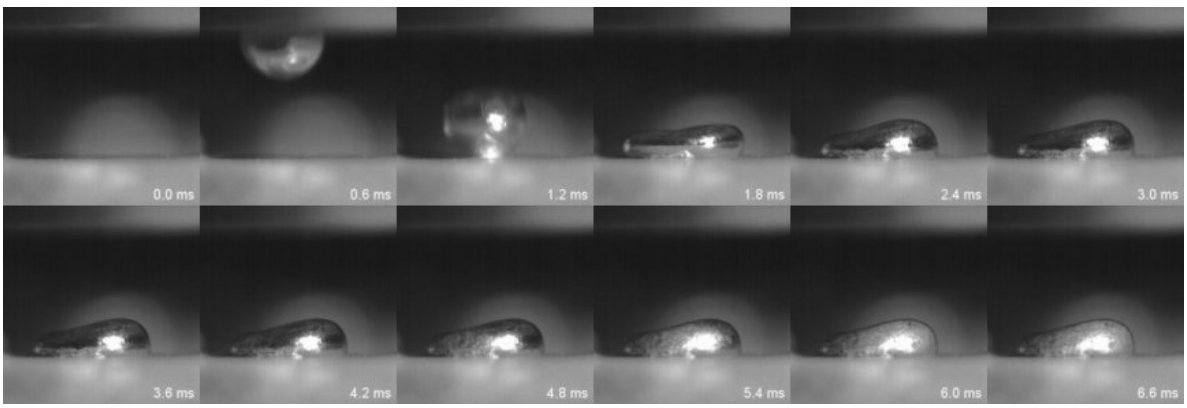

Fig. 2: Highspeed images of CuSn11 brazing sphere detachment, $d_{substrate,\ Ag}$ = 0.01 mm , flight phase and solidification, P_{laser} = 100 W, p_{N2}= 75 mbar, $d_{laser,irradiation\ droplet}$= 155 µm, $d_{brazing\ sphere}$= 0.6 mm, frame rate = 10,000 fps

The evaluation of the solidification process for Ag substrate and CuSn11 spheres with a diameter of 600 µm is shown in Figure 3. It can be seen, that there is a general trend towards lower solidification times for increasing substrate thicknesses. This effect can be related to the thermal mass underneath the solidifying

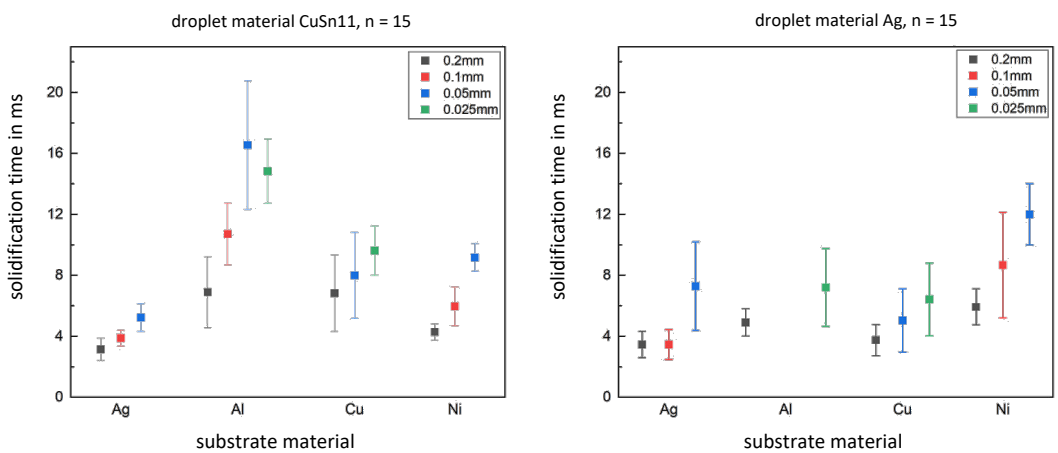

Fig. 3: Comparison of solidification times on different substrate materials with different thickness for CuSn11 and Ag with a droplet sphere diameter $d_{droplet}$ = 600 µm, n =15

droplet. For both sphere materials, Ag as substrate leads to the fastest solidification. This factor can be related to the highest thermal conductivity of Ag compared to the other materials. Especially for the experiments with CuSn11, Nickel does not show the highest solidification times as supposed from the data given in Table 1. This effect ca be related to good wetting properties compared to other combinations, like CuSn11 and Al, where the droplet is only partly connected to the substrate and therefore the heat dissipation into the substrate is decelerated. Due to the lower heat capacity and the higher heat conductivity of Ag compared to CuSn11 the overall solidification times are lower.

Besides the determination of the solidification time of the droplets also the reliability of the process was assessed by an optical inspection of the braze joints after the process. A successful joint is defined as a joint that does not directly fall off the substrate after or during the process, visible in the highspeed images. For certain material combinations it was observed, that there were no successful joints created. As a result, the solidified droplets directly fell off the substrate material. A statistical overview of this effect is given in Figure 4 for both brazing materials separately.

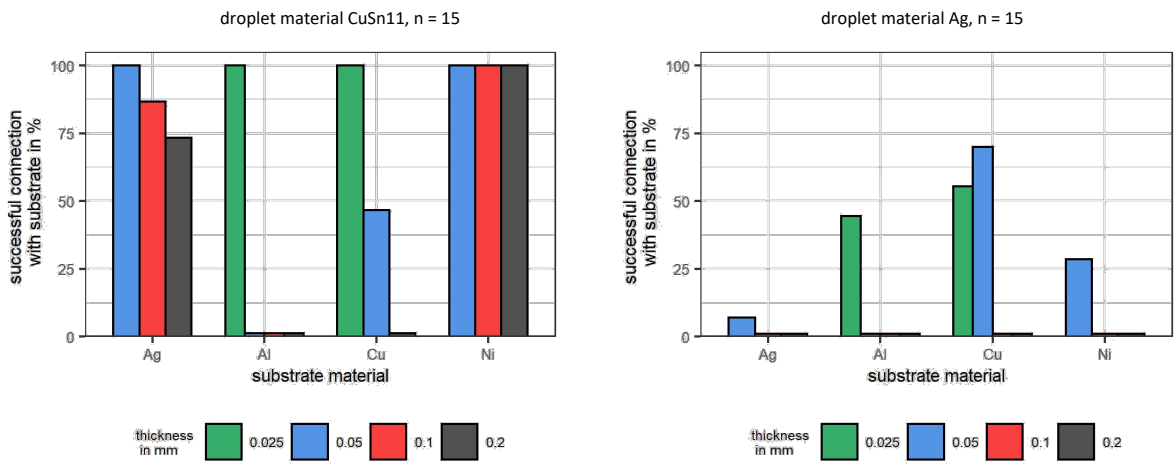

Fig. 4: Statistics for successful contacted substrates according to the evaluation of highspeed images; left: droplet material CuSn11; right: droplet sphere material Ag, n ≥ 9

For contacting the different substrates with CuSn11 as a droplet material it can be seen, that contacting was possible on every substrate. It is also noticeable, that for smaller substrate thicknesses the probability for a successful connection increase. For Al and Cu as a substrate material the chances for a successful connection decreases significantly for increasing substrate thicknesses. Especially for the combination of CuSn11 with Ni for all tested substrate thicknesses it was possible to create successful connection according to the evaluation before the shear testing. For Ag as droplet sphere material it can be seen, that firm connections on different substrates were hardly produced. The general trend for a higher susceptibility to generate joints on thinner substrates can be also observed for this case. The effect of better joining results on thinner substrates can be related to the slower solidification times, that have been evaluated in Figure 3. This improves the diffusion process, which is mainly limited by time and temperature. The thermal expansion coefficient of both droplet materials is comparable, so that it can be assumed that the poor joining results are mainly due to metallurgical effects and higher cooling rates of the Ag droplet.

4.2. Mechanical characterization by shear testing

To gain quantitative information on the mechanical performance of the brazed joints shear test were carried out and the sheared areas were measured. The results are displayed in Figure 5. For most material combinations that were not successful joinable according to Figure 4, it was not possible to measure proper shear stresses. For the results without error bar the maximum shear forces are not indicating the force that has to be applied to remove the droplet from the substrate since the foils are tearing apart. For this data points the resulting shear stresses must be even higher. Compared to Figure 3, a relation between higher

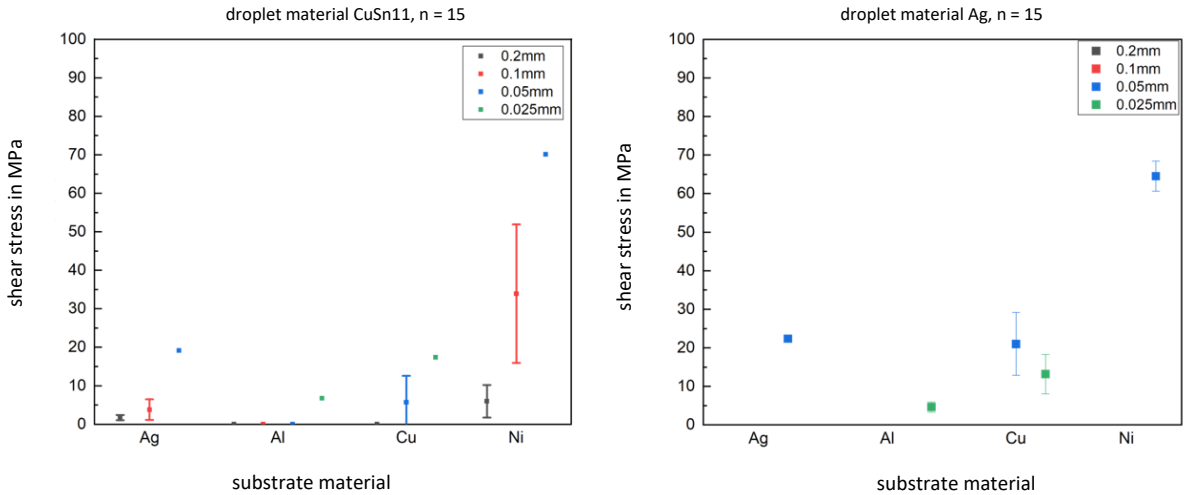

Fig. 3: Determined shear stresses according to DIN-EN 62137 1-2 of the created joints on different substrate materials; left: brazing sphere material Ag; right: brazing sphere material CuSn11; data points without error bar and shear stresses higher than 0 MPa indicate failures of the substrate but not in the joint.

solidification times and higher measured shear stresses can be found. This trend is analog to the results for successful connection from the evaluation of the highspeed imaging. The thinner the substrate of one material the higher the mechanical stresses that the joint can withstand. For CuSn11 it was possible to generate firm joints on each type of substrate, as long as the thickness of the substrate is below a certain level. For Ni substrate, the shear stresses on average per thickness are the highest. This effect is supposed to be related to the formation of low melting intermetallic Ni-Sn phases [14]. Especially on Al as substrate material comparably low shear stresses were measured, despite the solidification times being the highest for CuSn11 as droplet material. For Ag as droplet material the production of firm joints is much more limited than for CuSn11.

4.3. Metallurgical analysis of the joints

To gain deeper insights in the processes that take place on a metallurgical level, cross-sections have been by EDX- measurements, as can be seen in Figure 6. For the combination of CuSn11 as Droplet material and Ag as substrate material it can be seen in the cross-section, that there is a zone, where both materials are molten and Ag can be found multiple microns in the droplet material. In this region the melting process of the substrate by the heat input of the droplet is supposed to be beneficial for joining, since the process is not only limited by solid-liquid diffusion, but liquid-liquid diffusion, which is significantly faster than a solid-solid

diffusion process. For the combination of CuSn11 and Al it can be seen, that there is an irregular gap between the two joining partners. This effect is related to poor wetting behaviour between both materials. However, there is a small zone, where melting of Al by the heat input of CuSn11 is apparent. Since Al is highly susceptible for building oxide layers, a melting process in the joining zone is hindered mostly, due to the high melting point of Al-oxides.
In the joining zone of Ni and CuSn11 there is hardly any visible interruption between both joining partners. Compared to the other two cross-sections, there is no melting of the Ni visible. This effect is supposed to be mainly limited by the higher melting point of Ni compared to the other substrates.

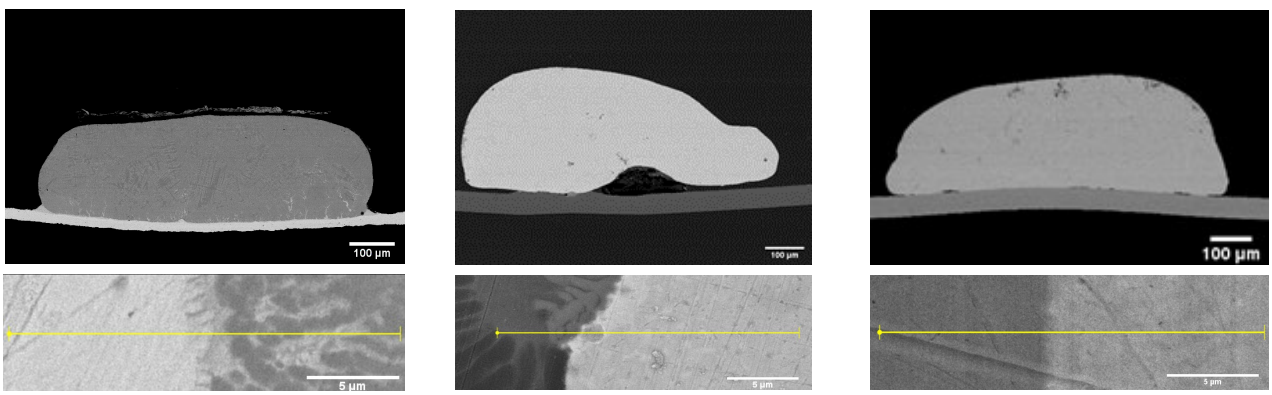

Fig. 6: REM images of cross-sections of joints with different material combinations; left: CuSn11 on Ag $d_{substrate}$ = 50 µm, middle: CuSn11 on Al $d_{substrate}$ = 100 µm, right: CuSn11 on Ni $d_{substrate}$ = 100 µm; bottom row shows magnification joint area

In Figure 7 an EDX mapping of the joining zones from Figure 6 are shown. For the combination of CuSn11 as droplet material with Ag or Al as substrate material melting of the substrate can be observed. This effect is related to a liquid droplet temperature that is higher than the melting temperature of the substrate. For Ni this effect is not observed since it is supposed, that the liquid temperature of the molten droplet is lower than the melting point of Ni. In this case intermetallic phases with low liquid temperature are supposed to form

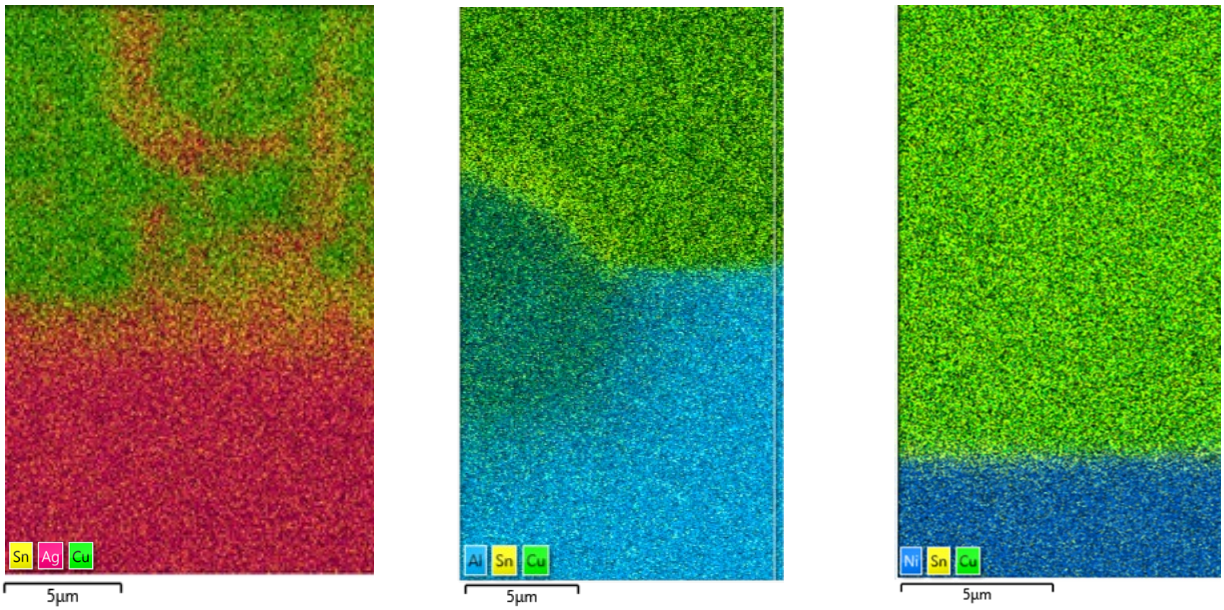

Fig. 7: EDX images of cross-sections of joints with different material combinations; left: CuSn11 on Ag $d_{substrate}$ = 50 µm, middle: CuSn11 on Al $d_{substrate}$ = 100 µm, right: CuSn11 on Ni $d_{substrate}$ = 100 µm;

In Figure 8 the determined shear stresses are plotted over the solidification time of the droplet on the substrate. It is noticeable that for increasing solidification times the maximum shear stresses that were obtained for different droplet substrate-droplet combinations increase, too. This is indicated by the red dashed line. This effect is mainly valid for droplet-substrate combinations that were successful joinable since poor wetting behaviour might influence the cooling conditions of the droplet, due to a lack of interconnection and therefore reduced heat flow. Depending on the materials and the solidification time it is possible to estimate process limits for a certain required shear stress.

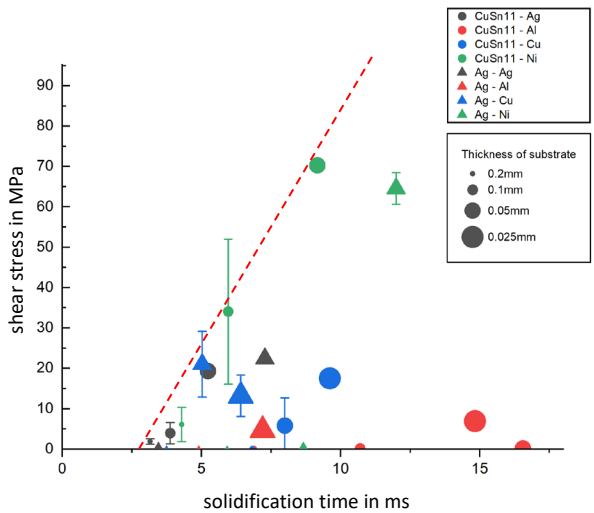

Fig. 8: Shear stress plotted over the solidification time for all material combinations and substrate thicknesses that have been evaluated in the course of this paper

5. Conclusion

In the scope of this paper it was found out, that the laser-based droplet brazing process is limited by multiple effects. One general aspect is the metallurgical compatibility between the joining partners. As long as there is poor wettability in the joining zone, it was not possible to establish successful joints. If the metallurgical compatibility is high, an increase of the measured shear stress was detected for increasing solidification times. This effect could be shown by contacting on thin substrates, to slow down the heat dissipation and to improve the diffusion process between the joining partners. However, it was also found out, that for some material combinations the joining process is dominated by liquid-liquid diffusion processes. This effect can only take place when the temperature of the droplet is higher than the liquid temperature of the substrate material and might be beneficial for the mechanical properties. It is also supposed, that intermetallic phases with low melting point are beneficial when it comes to contacting on thicker materials.

Depending on the solidification times and the measured shear stresses for different material combinations it is possible to define thermodynamic limitations of the process. This knowledge can be used to estimate the chances for a stable process for future applications, where materials or geometrical dimensions of the droplet or the substrate change.

6. Acknowledgements

This work is a result of the project “Development of a laser-assisted droplet-Jetting-Brazing-Technology for the expansion of process limits of conventional wire-bonding-applications for mounting and joining technology” which was founded by the German Research Foundation (DFG) within the Transregio 39. The authors gratefully acknowledge funding of the German Research Foundation (DFG) as well as support by the

Erlangen Graduate School in Advanced Optical Technologies (SAOT) by the Bavarian State Ministry for Science and Art.

7. References

[1] E. L. Dreizin, 'Droplet welding: A new technique for welding electrical contacts', *Weld. J. Miami Fla*, vol. 76, no. 4, pp. 67–73, Apr. 1997.

[2] T. Kokalj, J. Klemenčič, P. Mužič, I. Grabec, and E. Govekar, 'Analysis of the Laser Droplet Formation Process', *undefined*, 2006, Accessed: May 17, 2021. [Online]. Available: /paper/Analysis-of-the-Laser-Droplet-Formation-Process-Kokalj-Klemen%C4%8Di%C4%8D/68430ca3a9320aa0aaa1cadc41bb83bec9c133e3

[3] E. Govekar, A. Jerič, M. Weigl, and M. Schmidt, 'Laser droplet generation: Application to droplet joining', *CIRP Ann.*, vol. 58, no. 1, pp. 205–208, 2009, doi: 10.1016/j.cirp.2009.03.005.

[4] A. Jeromen, A. Kuznetsov, and E. Govekar, 'Laser Droplet Generation from a Metal Foil', *Phys. Procedia*, vol. 56, pp. 720–729, 2014, doi: 10.1016/j.phpro.2014.08.079.

[5] C. Held, U. Quentin, J. Heberle, F.-J. Gürtler, M. Weigl, and M. Schmidt, 'Laser Droplet Brazing for the Electrical Contacting of Composite Materials with Integrated Active Elements', *Phys. Procedia*, vol. 39, pp. 585–593, 2012, doi: 10.1016/j.phpro.2012.10.077.

[6] E. Zakel, T. Teutsch, G. Frieb, G. Azdasht, and J. Kurz, 'Laser Solder Jetting in Advanced Packaging', p. 8, 2003.

[7] T. Oppert, E. Zakel, and T. Teutsch, *A roadmap to low cost flip chip and CSP using electroless Ni/Au*. 1998, p. 113. doi: 10.1109/IEMTIM.1998.704534.

[8] F. Seigneur, Y. Fournier, T. Maeder, and J. Jacot, 'Laser soldering of piezoelectric actuator with minimal thermal impact', p. 10.

[9] S. Stein *et al.*, 'Experimental and numerical investigations regarding laser drop on demand jetting of Cu alloys', *Prod. Eng.*, vol. 11, no. 3, pp. 275–284, Jun. 2017, doi: 10.1007/s11740-017-0737-4.

[10] S. Stein, T. Weber, A. Winkler, M. Schmidt, and M. Gude, 'Investigations on laser assisted wire bonding by means of droplet joining of novel thermoplastic compatible piezoceramic modules', p. 2.

[11] M. Flössel, S. Gebhardt, A. Schönecker, and A. Michaelis, 'Development of a Novel Sensor-Actuator-Module with Ceramic Multilayer Technology', *Fraunhofer IKTS*, vol. 1, Sep. 2010, doi: 10.4416/JCST2010-00010.

[12] S. Stein, 'Laser Drop on Demand Micro Joining for High Temperature Wire Bonding Applications – System Technology And Mechanical Joint Performance', *J. Laser MicroNanoengineering*, vol. 12, no. 3, Dec. 2017, doi: 10.2961/jlmn.2017.03.0012.

[13] S. Stein *et al.*, 'Flight trajectory analysis of CuSn-droplets generated by laser drop on demand jetting, using stereoscopic high-speed imaging', *Opt. Express*, vol. 26, no. 8, p. 10968, Apr. 2018, doi: 10.1364/OE.26.010968.

[14] C. Schmetterer, H. Flandorfer, K. W. Richter, and H. Ipser, 'Phase Equilibria in the Ag-Ni-Sn System: Isothermal Sections', *J. Electron. Mater.*, vol. 36, no. 11, pp. 1415–1428, Oct. 2007, doi: 10.1007/s11664-007-0205-6.